Impedance Control of a Transfemoral Prosthesis using Continuously Varying Ankle Impedances and Multiple Equilibria

Namita Anil Kumar[1], Woolim Hong[1], and Pilwon Hur[2]

Abstract— Impedance controllers are popularly used in the field of lower limb prostheses and exoskeleton development. Such controllers assume the joint to be a spring-damper system described by a discrete set of equilibria and impedance parameters. These parameters are estimated via a least squares optimization that minimizes the difference between the controller's output torque and human joint torque. Other researchers have used perturbation studies to determine empirical values for ankle impedance. The resulting values vary greatly from the prior least squares estimates. While perturbation studies are more credible, they require immense investment. This paper extended the least squares approach to reproduce the results of perturbation studies. The resulting ankle impedance parameters were successfully tested on a powered transfemoral prosthesis, AMPRO II. Further, the paper investigated the effect of multiple equilibria on the least squares estimation and the performance of the impedance controller. Finally, the paper uses the proposed least squares optimization method to estimate knee impedance.

I. INTRODUCTION

The field of prosthesis design has been growing considerably over the past years, addressing the needs of both transtibial and transfemoral amputees [1]–[3]. Upon understanding the limitations of passive prostheses, researchers have made strides to develop powered prostheses [4]–[13]. These prostheses implement control strategies that fall into two major groups: impedance controllers that attempt to mimic human joint impedance [7], [14] and trajectory-tracking controllers that follow optimized joint trajectories [10], [15]–[17]. Of the two classes, the former has displayed greater promise in mimicking human-like gait kinetics. As stated in [7], an impedance controller enables the user to interact with the device much like in the case of healthy walking. An impedance controller consists of parameters pertaining to stiffness, damping and the equilibrium angle of the joints. By modulating these parameters, the joint torque required for support and propulsion of the human body can be generated. According to [7], researchers sectioned the gait cycle into 4-6 phases based on kinematic changes observed in a healthy human gait cycle (refer Fig. 1). Each phase has a set of three constant values–stiffness, damping, and the equilibrium angle. These values were initially estimated using a least squares optimizer that reduced the error between the torque of the impedance controller and human torque data

[1]Namita Anil Kumar and Woolim Hong are with the Department of Mechanical Engineering, Texas A&M University, College Station, TX 77843, USA {namita.anilkumar,ulim8819}@tamu.edu

[2]Pilwon Hur is with faculty of the Department of Mechanical Engineering, Texas A&M University, College Station, TX 77843, USA pilwonhur@tamu.edu

[18]. During testing, these estimates were tuned. Though successful, this approach mandated the manual tuning of several parameters. The study [19] implemented a series elastic actuator to modulate the impedance of the ankle joint in a transtibial prosthesis. Assuming the ankle to be a spring-damper system, the study estimated the stiffness parameters using a least squares optimization approach. The study, [20], proposed an ankle-foot exoskeleton that aided stroke patients in combating foot-drops. The system was manipulated using an impedance controller that was automatically tuned using a simple algorithm. Other notable attempts at estimating joint impedance during walking are [21] and [22]. The former proposes quasi-stiffness, which estimates joint stiffness by calculating the slope of the torque vs. angle curve during stance. The latter solved a constrained optimization problem where the joint impedance was the decision variable and the dynamics of a humanoid bipedal served as constraints. A common attribute of these studies is that the estimated impedance does not vary smoothly and continuously throughout the gait cycle. This paper will refer to the above group of estimation methods as *theoretical approaches*.

In the field of science, the most accepted method of identifying a system's parameters is via experiments by inducing perturbations. This paper will refer to such methods as *empirical approaches*. With the objective of empirically determining the ankle impedance while walking, researchers conducted experimental studies on the ankle [23]–[25]. These studies perturbed the ankle at various instances of the gait cycle. The ankle's response to the perturbation was gathered and analyzed to evaluate empirical values for stiffness and damping. It was reported that the ankle stiffness increases upon heel-strike until terminal-stance, following which the stiffness reduces until toe-off and maintains an almost constant value during swing phase. The damping parameter was observed to be high during heel-strike and toe-off. Unlike the results of many *theoretical approaches*, the *empirical* impedance parameters varied continuously and
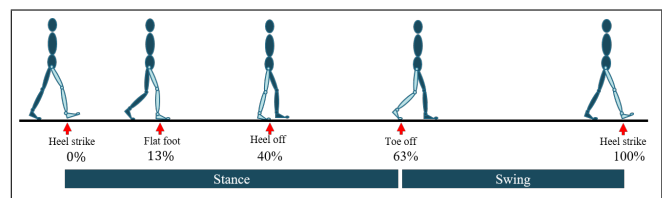

Fig. 1.   Gait cycle with important kinematic changes

smoothly throughout the gait cycle. The first objective of this paper is to bridge the gap between the *theoretical* and *empirical approaches* by extending the least squares method proposed by [7] to produce results that conform to the trends reported in [23]–[25]. Specifically, the stiffness and damping parameters will be allowed to vary continuously throughout the gait cycle. But, it must be emphasized that these estimates are solely for the purpose of designing impedance controllers and will differ, in magnitude, from those of healthy human walking.

In [14], researchers successfully implemented nonlinear impedance parameters to control the ankle and knee of a transfemoral prosthesis. The ankle's equilibrium angle and knee stiffness varied as a function of the vertical force measured by a load cell. Unfortunately, to the authors' knowledge, there have been no published attempts at *empirically* estimating knee or hip impedance during the gait cycle via perturbation studies. Any insight gained in this matter is limited to the swing phase [26]. Possible reasons for this gap in knowledge are (i) the huge investment required to conduct perturbation studies, and (ii) the grand challenge of isolating the effects induced by the perturbation to the joint being studied. Thus, the research community would highly benefit from *theoretical approaches* to estimating impedance. It is expected that the least squares optimization method proposed in this study can be used to estimate the required knee and hip impedance for impedance control in assistive devices. The concluding section of this paper presents a preliminary estimate of knee impedance. The resulting impedance will be compared with other literary works.

A recent study by [27] proposed a continuum of equilibria in contrast to the discrete set of equilibria implemented in [7]. The study also estimated the impedance of the knee joint using a *theoretical approach*. This study has raised questions regarding the effect of multiple equilibria on the performance of impedance controllers. The second objective of this paper is to fill this gap in knowledge by investigating the role of multiple equilibria on the proposed least squares estimation method. The validity of the resulting impedance will be assessed via implementation on an existing prosthesis AMPRO II. Additionally, attempts will be made to reduce the required tuning process during implementation.

II. LEAST SQUARES ESTIMATION OF IMPEDANCE PARAMETERS

The optimization problem solved in this paper is fundamentally similar to the one used by [7]. The lower limb joints are modeled as a spring-damper system. Let K and D represent the stiffness and damping of the joint, respectively. The generated torque can be calculated as follows.

$$\tau = K(\theta - \theta_{eq}) + D\dot{\theta} \qquad (1)$$

In (1), θ and $\dot{\theta}$ signify the position and velocity of the joint, while θ_{eq} is the equilibrium angle of the joint. It is desired that the generated torque be similar to that found in healthy human walking [18], say τ_{data}. Thus, the optimization problem minimizes the error between the torque τ and

Set label	Sections of the gait cycle			
Set A	0% - 13%	13% - 40%	40% - 63%	63% - 100%
Set B	0% - 40%		40% - 63%	63% - 100%
Set C	0% - 60%			63% - 100%
Set D	0% - 100%			

τ_{data}. Per [23]–[25], the stiffness and damping parameters continuously vary throughout the gait cycle in a smooth manner. Most of the variation in the impedance parameters is observed during the stance phase, while the parameters adopt an almost constant value during the swing phase. To permit the continuous variation of stiffness and damping, while maintaining minimal decision variables, the stiffness and damping parameters were represented by polynomials during the stance phase. The orders of the polynomials were adjusted to get a better fit (i.e., reduce the difference between τ and τ_{data}). During the swing phase, the impedance parameters were assigned constant values: k_{swing} and d_{swing}. Supposing m and n represent the order of the stiffness and damping polynomials, the impedance parameters at any instant during the gait cycle are determined as follows.

$$K(t) = \begin{cases} \sum_{i=0}^{m} k_i t^i & \text{for } 0 \leq t < 0.63 \\ k_{swing} & \text{for } 0.63 \leq t \leq 1 \end{cases} \qquad (2)$$

$$D(t) = \begin{cases} \sum_{i=0}^{n} d_i t^i & \text{for } 0 \leq t < 0.63 \\ d_{swing} & \text{for } 0.63 \leq t \leq 1 \end{cases} \qquad (3)$$

Note that $t = 0$ is equivalent to 0% of the gait cycle, while $t = 1$ signifies 100% of the gait cycle. In accordance with [18], it is assumed that swing phase occurs at 63% of the gait cycle. Per the requirement for continuity in the impedance parameters, $k_{swing} = k_0$ and $d_{swing} = d_0$. Much like [7], the gait is sectioned based on kinematic changes, making θ_{eq} a set of angles. The optimization problem can be summarized as follows.

$$\min_{\theta_{eq}, k_i, d_i} \quad \|\tau_{data} - \tau\|_2 \qquad (4)$$

$$\text{Subject to:} \quad K(t) \geq 0 \qquad D(t) \geq 0 \qquad (5)$$

$$K(0) = K(1) \qquad D(0) = D(1) \qquad (6)$$

$$\text{Continuity at } K(0.63) \text{ and } D(0.63) \qquad (7)$$

$$|\Delta\tau/\Delta t| \leq c \qquad (8)$$

The constraints listed in (5) force the positivity of the impedance parameters. Further, (6) ensures that the parameters maintain continuity between gait cycles and at the stance-to-swing transition. The last constraint, (8), forces the resulting τ to be continuous using a Lipschitz constant, c. Additional bounds were added, as needed, to restrict the value of the equilibrium angles.
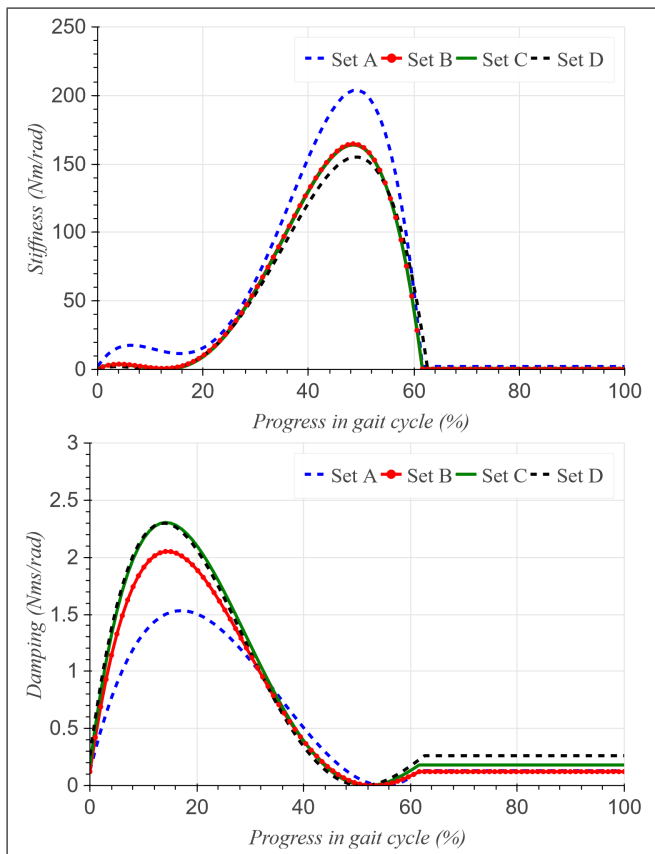
Fig. 2. Optimization results. **Top**: Stiffness curves, **Bottom**: Damping curves. The associated polynomial coefficients have been included in the Appendix (Table IV).

A. Multiple Equilibria

To study the impact of multiple equilibria on the impedance controller, four sets of equilibria were established. The first set echoes the one found in [7]. The gait cycle is sectioned in accordance with the foot contact sequence during the stance phase. The first phase initiates at heel-strike (0%) and continues until foot-drop (13%), followed by the second phase that terminates at heel-off (40%). The third phase exists between heel-off and toe-off (63%). Unlike [7], the swing phase of the gait cycle is not sectioned. This set of equilibria has been labeled as *Set A*. One of the objectives of this paper is to reduce the number of impedance control parameters that require tuning. The number of equilibria contributes heavily to the number of tuning parameters. Thus, in this paper, we expect to determine the minimum number of equilibria required to generate natural human-like walking (both kinematically and kinetically). The remaining three sets of equilibria implement fewer sections of the gait cycle. Table I lists said sets. The sectioning proposed in *Set B* is similar to the one proposed by [23].

B. Results of the optimization

The minimum order of the stiffness and damping polynomials required to lower the optimal cost was determined to be 4. This study fixed the order of the stiffness and damping polynomial to be the same. It was observed that the trend

Set label	0% - 13%	13% - 40%	40% - 63%	63% - 100%
Set A	0.0294	-0.3428	-0.3491	0.3029
Set B	-0.4258		-0.4363	0.0000
Set C	-0.4363			0.1453
Set D	-0.4655			

of the stiffness and damping parameters was not sensitive to the equilibria set. Fig. 2 depicts the stiffness and damping parameters. The corresponding torques, τ, has been presented in the Appendix. It is evident that all sets of parameters attained a suitable cost to the optimization problem. While the trend of the stiffness parameter, during stance, resembled that reported by [23]–[25], the values are considerably lower. The trend of the damping parameters, on the other hand, did not entirely conform to the results presented in [23]–[25]. Though it portrayed high damping post heel-strike, there is little to no damping during terminal-stance. Better results could be attained by increasing the order of the damping parameter or using a different optimizer. Yet, it must be noted that this optimization problem is concerned with fitting the torque generated by a simple spring-damper model to the torque generated by the overly redundant human body. Clearly, discrepancies are to be expected. The sole purpose of this problem is to design a controller that aids a mechatronic system emulate a human being.

Table II presents the equilibrium angles that resulted from the optimization. *Sets A* to *C* showed similarities by having the ankle plantarflexed during terminal-stance and dorsiflexed during swing. The plantarflexed angle helps store the potential energy needed for push-off. The dorsiflexed swing equilibrium angle ensures foot clearance to avoid trips. The equilibrium angle for *Set D* resembled a foot-drop condition–the state a human foot would conform to when physically unconstrained. It was anticipated that the foot-drop condition would pose a challenge during swing phase. It is likely that certain compensatory actions will be needed to ensure sufficient foot clearance during swing.

III. TESTING METHODOLOGY

The proposed sets of impedance parameters were tested on a custom-built powered transfemoral prosthesis shown in Fig. 3. AMPRO II (Fig. 3) has an actuated ankle and knee joint, and a passive spring-loaded toe joint. While the proposed impedance controller was implemented at the ankle, a previously published controller–a hybrid of impedance and trajectory tracking–was used to manipulate the knee. The latter has been discussed in [28]. The prosthesis was operated under a time-based scheme that utilizes a parameter that linearly increases from 0 to 1 as the gait progresses from 0% to 100%. This parameter is used to identify the progress in the gait cycle. A force sensor placed under the heel was used to initialize the parameter. To the authors' knowledge, current

state-based control schemes have limitations that are yet to be overcome [28], [29]. For instance, the study [29] investigated the usage of thigh angle as an indicator (or phase variable) of gait progression. It was demonstrated that the resulting phase variable does not display the ideal linear behavior during terminal-stance, making state identification difficult. Since the focus of this study was to evaluate the performance of continuously varying impedance parameters, it was preferred the performance be unaffected by the possible inaccuracies of state-based control. Further, it was unclear whether the stiffness at AMPRO II's toe joint would impact the ankle's performance. To study the effect of each impedance controller, in an isolated manner, the toe joint was restrained using a rigid element. Future studies will investigate the impact of toe stiffness on the generated gait.

A. Experimental protocol

To validate the proposed idea, an indoor experiment was designed using the aforementioned powered prosthesis in Fig. 3. A healthy young subject (male, 170cm, 70kg) participated in the experiment using an L-shape simulator that helped emulate prosthetic walking. The subject was asked to walk on a treadmill at his preferred walking speed (0.7 m/s). The subject's safety was assured by handrails located on either side of the treadmill. The experiment protocol has been reviewed and approved by the Institutional Review Board (IRB) at Texas A&M University (IRB2015-0607F).

B. Tuning

The recruited subject showed considerable height difference between his limbs while wearing the prosthesis. In an attempt to solve this issue, the subject was asked to wear boots during the experiments; unfortunately, the difference in height still persisted. This height difference significantly limited the amount ankle dorsiflexion observed in the prosthetic during mid-stance. In compensation, the
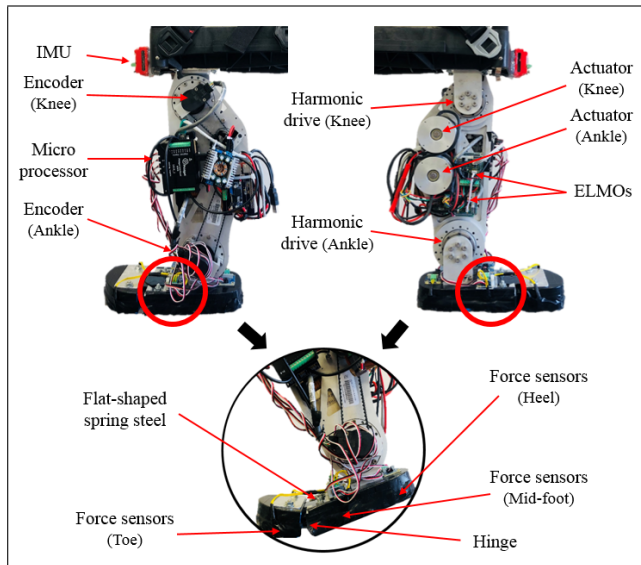

Fig. 3.   AMPRO II–a custom-built powered transfemoral prosthesis

TABLE III
THE TUNED SETS OF EQUILIBRIA IN RADIANS

Set label	0% - 13%	13% - 40%	40% - 63%	63% - 100%
Set A	0.0100	-0.0875	-0.3490	0.0873
Set B	-0.1745		-0.2617	0.0000
Set C	-0.2617			0.1452
Set D	-0.2617			

equilibrium angles were tuned to reduce the magnitude of the plantarflexed angles. The tuned equilibrium angles have been documented in Table III. In addition, the stiffness and damping curves were scaled down by factors α and β, respectively. This was done to limit the push-off assistance based on the participant's comfort and to abide by the motor's rated torque specifications. A major drawback of scaling was that the stiffness during swing phase was no longer sufficient to transition from the plantarflexed equilibrium angle during terminal-stance to the swing dorsiflexion angle. Thus, a constant stiffness term (γ) was uniformly added to the stiffness curve. The following equations describe the tuning process.

$$K_{tuned}(t) = \alpha K(t) + \gamma \qquad (9)$$
$$D_{tuned}(t) = \beta D(t) \qquad (10)$$

The scaling factors (α and β) were reduced until certain dorsiflexion was observed during the mid-stance phase. The term γ was increased until the ankle displayed dorsiflexion during the swing phase. Note that γ was not required for *Set D* since the equilibrium angle remained constant throughout the gait cycle. The stiffness curve for *Set A* was scaled by a factor of $\alpha = 0.4$, while $\alpha = 0.5$ for the remaining sets. Further, while $\beta = 0.2$ for *Set A*, $\beta = 0.166$ for the remaining sets. The constant term γ was equal to 20 for all sets. These scaling factors will change based on the subject. In the case of emulator studies, the subject's center of mass is displaced from the frontal plane–forcing the subject to adopt a cautious gait to avoid instabilities. Thus, the stiffness and damping curves are scaled down considerably. On the other hand, the factors will likely be higher in the case of amputees due to the center mass being located closer to the frontal plane. Though *Set D* did not necessitate a constant term, the term was implemented in the interest of conducting a systematic study where the stiffness curves of each set were approximately of same magnitude.

IV. RESULTS AND DISCUSSION

Figure 4 presents the average angular trajectory, torque, and power of the ankle for all four sets of impedance parameters. The averaged values represent 15-20 consecutive gait cycles. A Butterworth filter was used to process the data. The standard deviation was well-bounded, indicating the consistency of the observed results. Barring *Set D*, the trend of the kinematic and dynamic curves are similar across the impedance sets. The trend also bears a resemblance to healthy human data reported in [18].
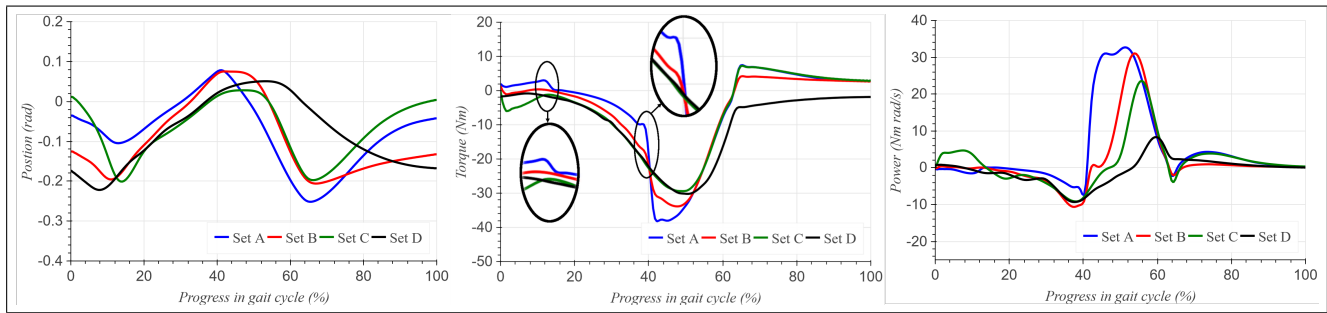
Fig. 4. Averaged results of the experiments. **Left:** Ankle angle, **Middle:** Ankle torque, and **Right:** Ankle power. The sections of the torque curve corresponding to foot-drop and heel-off have been enlarged.

On the other hand, the magnitude of the results was substantially lower in comparison. It is strongly believed that the height difference explained in Section III-B is the key reason behind these discrepancies. The following subsections compare the performance of each impedance set in terms of kinematics and dynamics of the generated gait. Following which, the limitations of this study have been discussed.

A. Comparison of kinematics

It should be emphasized that the stiffness and damping curves portrayed similar trends across all sets of impedance. Thus, the kinematics of the generated gait was dictated by the equilibrium angles. The following observations form the basis of this claim: (i) *Set A* displayed lesser plantarflexion proceeding heel-strike in comparison to the other sets owing to the dorsiflexed equilibrium angle between heel-strike and foot-drop. *Set C* displayed foot slap (steep plantarflexion) proceeding heel strike. Increasing damping could counter this issue. (ii) Lesser dorsiflexion was observed during terminal-stance in *Set C* and *D*. Unlike these sets, *Set A* and *B* increase the plantarflexed equilibrium angle in increments. It is likely that such an incremental ascension assisted the subject in achieving higher dorsiflexion during mid- and terminal-stance (iii) The variance in ankle angles, among sets, at the beginning and end of the gait cycle is due to varying swing equilibrium angles. It would be beneficial to implement a higher swing equilibrium angle since it ensures sufficient foot clearance during swing (iv) Plantarflexion at push-off was greater in *Set A* due to the higher equilibrium angle. Additionally, *Set A* showed an earlier descent from dorsiflexion to plantarflexion at heel-off (40%). A plausible explanation is that the combined effect of heightened stiffness and higher plantarflexion forced an earlier push-off (v) Evidently, *Set D* showed an absence of dorsiflexion during swing phase due to the plantarflexed equilibrium angle. As anticipated, the foot-drop equilibrium angle of *Set D* resulted in few stumbles during the swing phase [30].

A kinematic abnormality that cannot be overlooked is the absence of push-off in *Set D*. As stated earlier, the impedance control strategy was implemented using a time parameter that linearly increased as the gait progressed. With that being said, the success of time-based control heavily depends on the subject's ability to synchronize his/her gait with the time parameter. This synchronization task proved to be a mighty

challenge while testing *Set D*. Specifically, the constant foot-dropped equilibrium angle introduced gait abnormalities such as exaggerated hip extension at toe-off. In preparation for the over-extended hip angle, the subject forcibly maintained a dorsiflexed ankle beyond peak stiffness (which occurs at 50% of the gait cycle). When toe-off eventually occurred, the stiffness was thus insufficient to quickly restore the ankle to the plantarflexed equilibrium.

B. Comparison of dynamics

Set A and *B* resulted in higher torque during terminal-stance in comparison to the other sets. This is likely due to higher dorsiflexion in mid and terminal-stance (as discussed in Section IV-A). As a consequence, the corresponding power was higher in *Set A* and *B*. Most interesting to note was the abrupt change in the torque corresponding to *Set A* at foot-drop (13%). Such a change was not observed in the results of the other sets. This is undoubtedly a consequence of the change in *Set A*'s equilibrium angle at foot-drop. Similar behavior was observed at heel-off (40%) in the results of both *Set A* and *B*. Thus, fewer changes in equilibrium angles ensure a smoother torque output. Further, the re-positioning of the ankle joint to the swing dorsiflexed angle resulted in positive torque at the beginning of the swing phase for *Sets A* to *C*. In regards to the power curves, *Set A*'s power output displays an aberrant increase at heel-off. The backing rationale is the high velocity arising from the hastened push-off detailed in Section IV-A. Finally, the push-off power associated with *Set D* was significantly lower due to the previously discussed delayed push-off.

C. Limitations of this study

The aforementioned height difference between the subject's limbs forced him to adopt a limb; i.e., a shorter step length and longer stance phase on the limb without the prosthetic. A major drawback of these gait asymmetries was insufficient loading of the prosthetic ankle during mid-stance; resulting in the reduced dorsiflexion. Further, the swing equilibrium angle could have been tuned in a more systematic manner; i.e., the imposed swing dorsiflexed angle could have been uniform across all sets. Finally, the usage of time-based control enforced the stringent requirement of gait synchronization on the subject.

V. CONCLUSION

This study proposed a least squares approach to estimating ankle impedance based on the work of [7] for the purpose of designing impedance controllers. The resulting stiffness values followed a trend consistent with perturbation studies [23]–[25]. The estimated impedance parameters were not sensitive to the number of equilibria enforced. On studying the effect of multiple equilibria on the impedance controller's performance, the following results were revealed: (i) Multiple equilibria during the mid and terminal-stance phase that increase the plantarflexed equilibrium angle (in increments) can assure more ankle dorsiflexion during mid-stance. Consequently, the generated torque and power at push-off are higher (ii) Abrupt changes in torque can be expected at the instances when the equilibrium angle switches. Such changes impact the robustness of the system to perturbations. This ideology is the motivation behind studies in continuum of equilibria [27] (iii) While overly plantarflexed equilibrium angle during terminal-stance results in higher push-off torque, it can give rise to premature push-off (iv) Most importantly, a single equilibrium angle during stance phase is sufficient to generate human-like kinematics and dynamics at the cost of lower mid-stance dorsiflexion and foot slap at heel-strike. Amputee studies will be conducted to identify the most suitable equilibria set based on the observed kinematics, kinetics, and metabolic cost.

VI. FUTURE WORK

To overcome the above-listed limitations, a state-based control scheme will be implemented to enable flexibility in gait speed. The basis of such a control scheme can be found in [28]. Current efforts are targeted at overcoming the limitations of the control scheme by using sensor-fusion. This paper assumed the order of the stiffness and damping polynomials to be the same during the stance phase. Future attempts will investigate the validity of this assumption. Presently, a height adjustable prosthesis is under development. This prosthesis will be used in all future studies of the impedance controller. Based on this study, an automated tuning algorithm will be developed and consecutively implemented on a transfemoral prosthesis. The dorsiflexion observed during mid-stance will serve as the primary indication of well-tuned stiffness and damping parameters. Further, the impedance parameters proposed in this study will be used in a hybrid control strategy that would implement impedance control during the stance phase followed by trajectory tracking during swing [28].

In regards to the knee, a preliminary estimation of knee impedance during stance has been presented in Fig. 5. The estimation utilized the sectioning proposed in *Set B*. The optimized equilibrium angles were 0.1413 rad of knee flexion during initial stance, followed by 0.1968 rad until toe-off. The result is consistent with the values implemented by [7] and [27]. Considering the extensive knee movement during swing, it may be more desirable to use trajectory tracking during swing. Another path worthy of investigation is the concept of a continuum of equilibria proposed by [27]. For starters, one could implement a polynomial curve fitted to the current discrete equilibria.

APPENDIX

The following figure depicts the fit attained using the least squares optimization. Also included is human torque data from [18]. Table IV presents the optimized coefficients of the stiffness and damping polynomials.

Fig. 6. The torque τ generated from the optimization in comparison to human torque data [18]

TABLE IV
THE COEFFICIENTS OF THE POLYNOMIAL CURVES

	Stiffness				
Set label	k_4	k_3	k_2	k_1	k_0
Set A	-29870.57	28322.46	-7061.82	586.04	2.21
Set B	-19977.92	17340.71	-3424.51	199.97	0.32
Set C	-19822.71	17146.19	-3333.05	181.16	0.75
Set D	-16520.32	14144.17	-2596.67	136.56	0.00

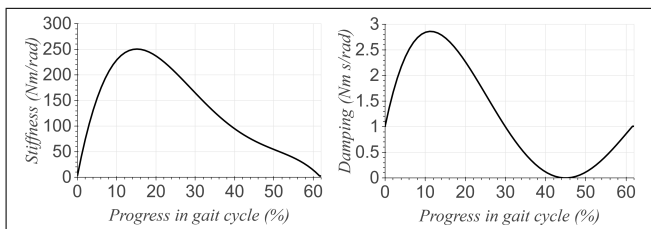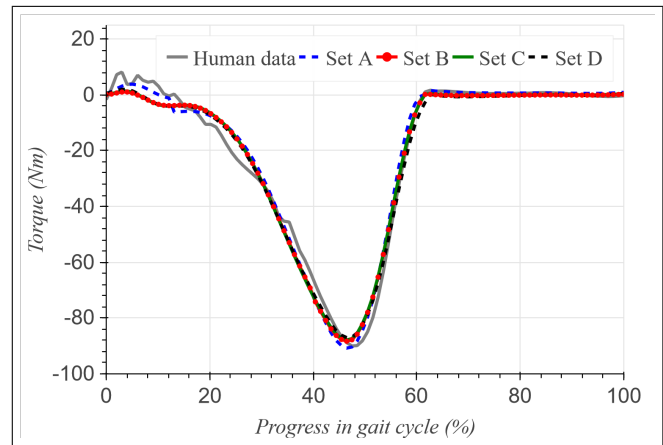|	Damping				
Set label	d_4	d_3	d_2	d_1	d_0
Set A	-22.45	88.08	-76.20	18.76	0.12
Set B	-140.21	261.35	-158.46	31.21	0.12
Set C	-164.32	303.05	-181.22	35.04	0.18
Set D	-171.23	311.36	-182.97	34.53	0.26

Fig. 5. Preliminary estimation of knee impedance using the proposed theoretical approach. The estimation was limited to the stance phase of the gait cycle. **Left:** Stiffness, **Right:** Damping

REFERENCES

[1] J. Perry, L. A. Boyd, S. S. Rao, and S. J. Mulroy, "Prosthetic weight acceptance mechanics in transtibial amputees wearing the single axis, seattle lite, and flex foot," *IEEE Transactions on Rehabilitation Engineering*, vol. 5, no. 4, pp. 283–289, 1997.

[2] S. Blumentritt, H. W. Scherer, U. Wellershaus, and J. W. Michael, "Design principles, biomechanical data and clinical experience with a polycentric knee offering controlled stance phase knee flexion: a preliminary report," *JPO: Journal of Prosthetics and Orthotics*, vol. 9, no. 1, pp. 18–24, 1997.

[3] D. Romo, "Prosthetic knees," *Physical medicine and rehabilitation clinics of North America*, vol. 11, pp. 595–607, vii, 2000.

[4] S. K. Au, H. Herr, J. Weber, and E. C. Martinez-Villalpando, "Powered ankle-foot prosthesis for the improvement of amputee ambulation," in *2007 29th Annual International Conference of the IEEE Engineering in Medicine and Biology Society*, Aug 2007, pp. 3020–3026.

[5] T. Lenzi, M. Cempini, J. Newkirk, L. J. Hargrove, and T. A. Kuiken, "A lightweight robotic ankle prosthesis with non-backdrivable cam-based transmission," in *2017 International Conference on Rehabilitation Robotics (ICORR)*, July 2017, pp. 1142–1147.

[6] E. C. Martinez- Villalpando, J. Weber, G. Elliott, and H. Herr, "Design of an agonist-antagonist active knee prosthesis," in *2008 2nd IEEE RAS EMBS International Conference on Biomedical Robotics and Biomechatronics*, Oct 2008, pp. 529–534.

[7] F. Sup, A. Bohara, and M. Goldfarb, "Design and control of a powered transfemoral prosthesis," *The International Journal of Robotics Research*, vol. 27, no. 2, pp. 263–273, 2008.

[8] N. Thatte and H. Geyer, "Towards local reflexive control of a powered transfemoral prosthesis for robust amputee push and trip recovery," in *2014 IEEE/RSJ International Conference on Intelligent Robots and Systems*, Sep. 2014, pp. 2069–2074.

[9] M. Windrich, M. Grimmer, O. Christ, S. Rinderknecht, and P. Beckerle, "Active lower limb prosthetics: a systematic review of design issues and solutions," *Biomedical Engineering Online*, vol. 15, no. 3, p. 140, 2016.

[10] H. Zhao, J. Horn, J. Reher, V. Paredes, and A. D. Ames, "First steps toward translating robotic walking to prostheses: a nonlinear optimization based control approach," *Autonomous Robots*, vol. 41, no. 3, pp. 725–742, 2017.

[11] V. Azimi, T. Shu, H. Zhao, E. Ambrose, A. D. Ames, and D. Simon, "Robust control of a powered transfemoral prosthesis device with experimental verification," in *2017 American Control Conference (ACC)*, May 2017, pp. 517–522.

[12] T. Elery, S. Rezazadeh, C. Nesler, J. Doan, H. Zhu, and R. D. Gregg, "Design and benchtop validation of a powered knee-ankle prosthesis with high-torque, low-impedance actuators," in *2018 IEEE International Conference on Robotics and Automation (ICRA)*, May 2018, pp. 2788–2795.

[13] A. F. Azocar, L. M. Mooney, L. J. Hargrove, and E. J. Rouse, "Design and characterization of an open-source robotic leg prosthesis," in *2018 7th IEEE International Conference on Biomedical Robotics and Biomechatronics (Biorob)*, Aug 2018, pp. 111–118.

[14] N. P. Fey, A. M. Simon, A. J. Young, and L. J. Hargrove, "Controlling knee swing initiation and ankle plantarflexion with an active prosthesis on level and inclined surfaces at variable walking speeds," *IEEE Journal of Translational Engineering in Health and Medicine*, vol. 2, pp. 1–12, 2014.

[15] R. D. Gregg, T. Lenzi, L. J. Hargrove, and J. W. Sensinger, "Virtual constraint control of a powered prosthetic leg: From simulation to experiments with transfemoral amputees," *IEEE Transactions on Robotics*, vol. 30, no. 6, pp. 1455–1471, 2014.

[16] V. Paredes, W. Hong, S. Patrick, and P. Hur, "Upslope walking with transfemoral prosthesis using optimization based spline generation," in *2016 IEEE/RSJ International Conference on Intelligent Robots and Systems (IROS)*, Oct 2016, pp. 3204–3211.

[17] A. E. Martin and R. D. Gregg, "Stable, robust hybrid zero dynamics control of powered lower-limb prostheses," *IEEE Transactions on Automatic Control*, vol. 62, no. 8, pp. 3930–3942, 2017.

[18] D. A. Winter, *Biomechanics and motor control of human movement*, 4th ed. Wiley, 2009.

[19] M. F. Eilenberg, H. Geyer, and H. Herr, "Control of a Powered Ankle-Foot Prosthesis Based on a Neuromuscular Model," *IEEE Transactions on Neural Systems and Rehabilitation Engineering*, vol. 18, no. 2, pp. 164–173, 2010.

[20] J. Blaya and H. Herr, "Adaptive Control of a Variable-Impedance Ankle-Foot Orthosis to Assist Drop-Foot Gait," *IEEE Transactions on Neural Systems and Rehabilitation Engineering*, vol. 12, no. 1, pp. 24–31, 2004.

[21] K. Shamaei, G. S. Sawicki, and A. M. Dollar, "Estimation of Quasi-Stiffness of the Human Knee in the Stance Phase of Walking," *PLOS ONE*, vol. 8, no. 3, 2013.

[22] Y. Hu and K. Mombaur, "Analysis of human leg joints compliance in different walking scenarios with an optimal control approach," *IFAC-PapersOnLine*, vol. 49, no. 14, pp. 99–106, 2016.

[23] E. J. Rouse, L. J. Hargrove, E. J. Perreault, and T. A. Kuiken, "Estimation of Human Ankle Impedance During the Stance Phase of Walking," *IEEE Transactions on Neural Systems and Rehabilitation Engineering*, vol. 22, no. 4, pp. 870–878, 2014.

[24] H. Lee, E. J. Rouse, and H. I. Krebs, "Summary of Human Ankle Mechanical Impedance During Walking," *IEEE Journal of Translational Engineering in Health and Medicine*, vol. 4, pp. 1–7, 2016.

[25] A. L. Shorter and E. J. Rouse, "Mechanical Impedance of the Ankle during the Terminal Stance Phase of Walking," *IEEE Transactions on Neural Systems and Rehabilitation Engineering*, vol. 26, no. 1, pp. 135–143, 2018.

[26] B. Koopman, E. H. Van Asseldonk, and H. Van Der Kooij, "Estimation of Human Hip and Knee Multi-Joint Dynamics Using the LOPES Gait Trainer," *IEEE Transactions on Robotics*, vol. 32, no. 4, pp. 920–932, 2016.

[27] A. Mohammadi and R. D. Gregg, "Variable impedance control of powered knee prostheses using human-inspired algebraic curves," *Journal of Computational and Nonlinear Dynamics*, vol. 14, pp. 1–10, 2019.

[28] W. Hong, V. Paredes, K. Chao, S. Patrick, and P. Hur, "Consolidated control framework to control a powered transfemoral prosthesis over inclined terrain conditions," in *2019 International Conference on Robotics and Automation (ICRA)*, May 2019, pp. 2838–2844.

[29] S. Rezazadeh, D. Quintero, N. Divekar, and R. D. Gregg, "A phase variable approach to volitional control of powered knee-ankle prostheses," in *2018 IEEE/RSJ International Conference on Intelligent Robots and Systems (IROS)*, Oct 2018, pp. 2292–2298.

[30] N. J. Rosenblatt, A. Bauer, D. Rotter, and M. D. Grabiner, "Active dorsiflexing prostheses may reduce trip-related fall risk in people with transtibial amputation," *Journal of Rehabilitation Research & Development*, vol. 51, no. 8, 2014.